

## SCALING OF FLUID FLOW VERSUS FRACTURE STIFFNESS

CHRISTOPHER L PETROVITCH\*, LAURA J. PYRAK-NOLTE†, AND DAVID D. NOLTE‡

**Abstract.** Finite-size scaling analysis applied to single fractures with weakly correlated aperture distributions reveals a fundamental scaling relationship between fracture stiffness and fracture fluid flow. Computer simulations extract the dynamic transport exponent, which is required to collapse the flow-stiffness relationships onto a universal scaling function. Near the critical percolation threshold, the scaling function displays two exponentially decaying regions whose transition point is governed by the multifractal spectrum of stressed flow paths. The resulting hydromechanical scaling function provides a link between fluid flow and the seismic response of a fracture.

**1. Introduction.** A non-intrusive geophysical technique to probe the hydraulic properties of rock fractures has long been sought by scientists and engineers. Such a technique would provide a new method to ascertain the effectiveness of subsurface projects such as the extraction of drinkable water, production of oil & petroleum, installation and monitoring of subsurface infrastructure and the storage of anthropogenic byproducts (CO<sub>2</sub>, nuclear waste, etc) in subsurface reservoirs. Extensive research has been performed on the laboratory scale to examine fluid flow through fractures, fracture geometry and deformation under stress as well as the seismic response of fractures. However, one of the fundamental tasks in geophysics is to relate fracture properties and processes at one length scale to properties and processes at other length scales. For example, in the laboratory, measurements are performed on fractured rock samples that range in size from 10<sup>-2</sup> – 10<sup>-1</sup> m with fracture apertures on the order of 10<sup>-6</sup> – 10<sup>-4</sup> m using seismic wavelengths on the order of 10<sup>-3</sup> – 10<sup>-2</sup> m. Conversely, at field scales, seismic frequencies from 1 Hz to 1 kHz illuminate regions on the order of 10<sup>3</sup> – 10<sup>1</sup> m. Thus the development of seismic methods that can delineate and characterize the hydraulic properties of fractures requires a fundamental understanding of the relationship between the hydraulic and mechanical properties of fractures and, more importantly, how this relationship scales with the size of the sampled region.

The ability to relate and scale the hydromechanical properties of fractures requires that both hydraulic and mechanical processes are controlled at similar length scales associated with fracture geometry (e.g. size and spatial distributions of aperture and contact area, surface roughness, fracture length, etc.). There have been many attempts to quantify the role of these geometric quantities with regard to fluid flow and deformation as a function of stress. For instance, [16] showed that the flow rates associated with fractures under normal load have three distinct behaviors as a function of stress. The first behavior occurs at low stresses, where flow rates obey the “cubic” law. However, as normal stress increases, the flow rate deviates from the cubic-law aperture dependence. Deviations from the cubic law were partially explained by using the dominant surface roughness wavelength to approximate the hydraulic aperture [19, 18]. Alternatively, a correction factor was constructed from the ratio of the first and second moments of the aperture distribution [10]. While these approaches focused on the void areas across the fracture plane, the contact area provides another approach. The fracture was modeled as a system of interacting circular obstructions confined to a plane [14]. The analytic solution for the flow around a circular obstruction of the given radii was used to compute the total flow rate through the fracture. This approach provided a stress-dependent flow rate, but the contact area was assumed to increase linearly with stress [15].

It has been shown experimentally that, at high stresses, the flow exponent should deviate from the “cubic” law [9]. Metal castings of natural granite fractures were made at stresses as high as 85 MPa. The castings showed large regions of void space connected by narrow tortuous channels [9, 5]. This experiment found that the large void spaces deformed significantly as the normal load increased, while narrow channels remained open because they were supported by adjacent contact area. From

---

\*Physics Department, Purdue University, IN ([cpetrovi@purdue.edu](mailto:cpetrovi@purdue.edu))

†Physics Department, School of Civil Engineering, and the Department of Earth and Atmospheric Sciences, Purdue University, IN ([ljpn@purdue.edu](mailto:ljpn@purdue.edu))

‡Physics Department, Purdue University, IN ([nolte@purdue.edu](mailto:nolte@purdue.edu))

these observations, the authors concluded that once the narrow paths dominate the fluid flow, the flow becomes approximately independent of stress. Following this study, a more unified numerical approach was taken that included both mechanical deformation and fluid flow [8]. Experimental flow-stiffness data for fractures that ranged in length from 0.05 m to 0.3 m suggested an empirical relationship between the hydraulic and mechanical properties that appeared to be controlled by the geometry of the void spaces and the contact area in the fracture. A strong dependence of flow on stiffness was observed, but the samples were of different aperture distributions and scale. An outstanding question is whether there exists a universal relationship between flow and stiffness when appropriate geometric length scales are taken into consideration.

In this letter, a finite-size scaling approach is presented that quantifies the scaling relationship between fluid flow and fracture specific stiffness for single fractures and numerically establishes that a universal hydromechanical function exists. The scale-dependence is removed by finding the critical transport scaling exponent that yields a universal scaling function.

**2. Methods.** Fractures with edge lengths that range from 0.0625 to 1 meter were simulated to span over an order of magnitude in length scale. A larger range in scale would be preferred, but is not computationally feasible at this time. By allowing the fracture size to vary, the data were expected to display both *critical* and *effective medium* regimes. A fracture is in the effective medium regime when the scaling of fluid flow can be described completely through the moments of the aperture distribution. It is in the critical regime when flow paths are tenuous, and flow is a non-trivial function of the scale and topology. To quantify these two regimes, percolation theory uses the void area fraction as the critical variable. In the critical regime, the flow-stiffness relation can be written in a finite-size scaling form as

$$(2.1) \quad q \propto L^{-t/\mu} F \left[ (\kappa - \kappa_c) L^{1/\mu} \right]$$

where  $q$ ,  $\kappa$ ,  $\kappa_c$  and  $L$  are the flow rate, fracture specific stiffness, critical specific stiffness, and scale, respectively. The exponents,  $\mu$  and  $t$ , are the 2D correlation exponent and the dynamic flow exponent, respectively. The 2D correlation exponent has a well-known value of 4/3 [12], but the flow exponent must be determined numerically. The function  $F$  is possibly a universal function that also is obtained numerically. The critical specific stiffness is defined as the stiffness of a fracture when the normal load has reduced the void area fraction to the critical area percolation threshold. Flow has the form of a power-law as the stiffness approaches the critical stiffness because the function  $F$  approaches a constant.

Three computational methods were used to study the flow-stiffness relationship: (1) a stratified percolation approach to generate aperture-scale (10 – 100 microns) fracture void geometry for fractures that span over an order of magnitude in fracture length (0.0625 to 1 m); (2) a combined conjugate-gradient solver and fast-multipole method for determining fracture deformation; and (3) a flow network model for simulating fluid flow, fluid velocity and fluid pressures within a fracture. To generate a fracture void geometry, the fracture plane was defined as a 512 x 512 array of pixels. Within this array, a “point” represented by 4x4 pixels was randomly added to the array (incrementing by one). Each pixel had a transverse scale of 1.95 mm. During random placement of the points within the array, points were allowed to overlap. The number of overlaps for each pixel within the array was equated to the aperture at that pixel. This created a fracture void geometry with transverse correlation lengths approximately equal to 1.95 mm and with a log-normal aperture distribution [7]. The aperture distributions were used to study the flow and deformation properties of the initial 512 x 512 aperture array and then sub-sectioned (Figure 1) down to 32 x 32 subsection (or scales from 1, 1/2, 1/4, 1/8, 1/16, 1/32 m) to study the effect of scaling on the flow-stiffness relationship. One hundred fractures were simulated at each scale to form the ensemble average values. The fluid flow calculations assumed the properties of water with the viscosity of 0.001 Pa seconds. The elastic properties of granite were assumed for the bulk rock (i.e., a Poisson ratio of 0.25 and Young’s modulus of 60 GPa [5]).

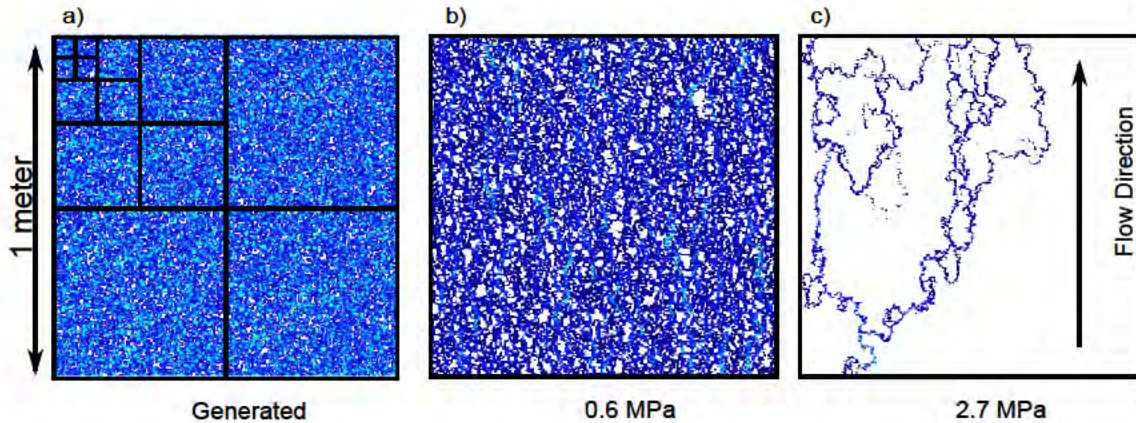


FIG. 1. (a) An example of a simulated weakly correlated fracture. The lines indicate the finite-sized subsamples. (b) Fluid velocity field at 0.6 MPa. (c) The same fracture fluid velocity field at 2.7 MPa normal load.

The generated fractures were numerically deformed under a normal load [4]. Each asperity was modeled as a standing cylinder, and the normal load was applied to an infinite half-space. Both the cylinders and the half-space were given the same material properties (that of granite) and both were allowed to deform elastically. Numerically, this system is represented by a set of linear equations, with each equation computing the deformation of a given asperity. The number of equations grows as the contact area of the fracture grows. The method was improved by iteratively solving the linear system and using the fast multipole method to speed up the matrix-vector multiplication [8]. The solver was modified to use periodic boundary conditions [6] to remove edge effects. Fluid flow rates were computed at each step in normal load by converting the aperture distribution to a network of elliptical pipes [13, 17, 2]. Ellipses were used to match the variation in aperture (row-wise) and then connected in the direction of the pressure gradient. The analytic solution to laminar flow in an elliptical pipe was used to generate a system of equations that represented the flow through the fracture plane. This model is preferred over a bi-lattice grid method because it is computationally more efficient (run-times are 4-10 times faster) and it was shown to model 2D micro-model experimental data more accurately [2]. Figure 1b shows the fluid velocity field under a small load (0.6 MPa), while Figure 1c shows it under a large load (2.7 MPa) where the “critical necks” of the fracture geometry are clearly apparent.

**3. Hydromechanical Finite-Sized Scaling.** The computed flow-stiffness relationships are shown in Figure 2a. Each curve represents a different physical scale. The finite-size effects are clearly observed, when stiffness increases, as a fan of curves. The dynamic flow exponent,  $t$ , must be determined to unravel the universal function in Equation 2.1 because it plays a key role in the first stage of the data collapse. This was completed by extrapolating the flow rate at threshold to the infinite size limit [11]. The flow exponent was determined to be  $t/\mu = 2.38$ . In Figure 2b the data are partially collapsed by scaling the flow rate by  $L^{t/\mu}$ , reflecting the pre-factor of the universal scaling function in Equation 2.1. This scaling also displays the fixed point near 5800 MPa/mm, where each of the flow-stiffness curves cross at a single point, meaning that flow and stiffness are scale invariant. The stiffness at this fixed point is defined as the critical stiffness,  $\kappa_c$ , used in Equation 2.1 and is also the average stiffness at the critical threshold. This value of critical stiffness is a key parameter in the second and final stage of data collapse.

To complete the data collapse, the stiffness axis was shifted by  $\kappa_c$  and scaled by  $(L/L_0)^{1/\mu}$ , as shown in Figure 3, while continuing to use  $q(L/L_0)^{t/\mu}$  as the scaled vertical axis. With this scaling, all the data at all scales fall on a single curve that has two clear regions with distinct slopes. The solid line on Figure 3 is shown to guide the eye and represents the universal function of Equation

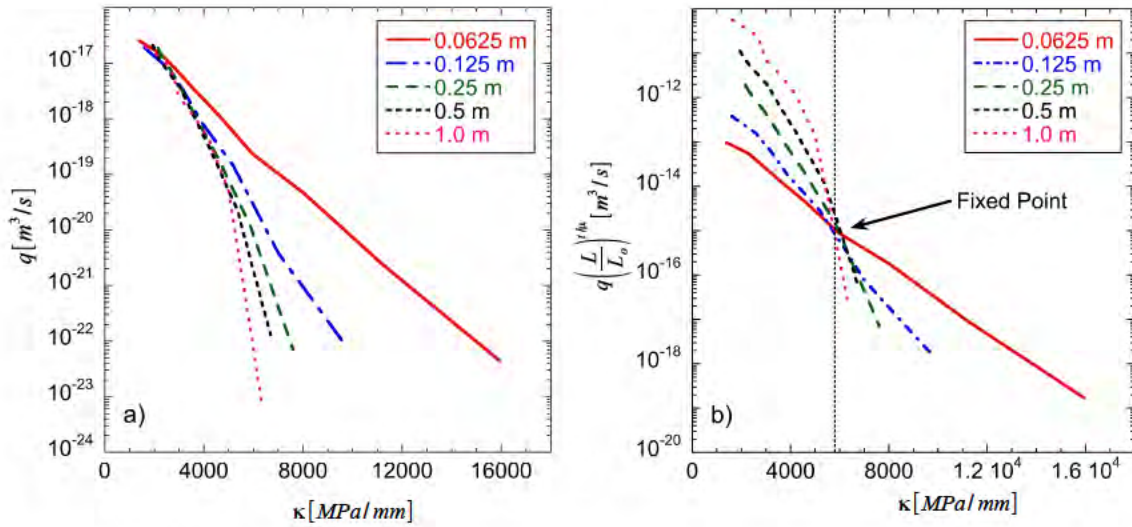


FIG. 2. (a) Raw flow-stiffness data, averaged for each scale. (b) A partial data collapse of the flow-stiffness relationship. The flow rate was scaled by  $(L/L_0)^{t/\mu}$ .

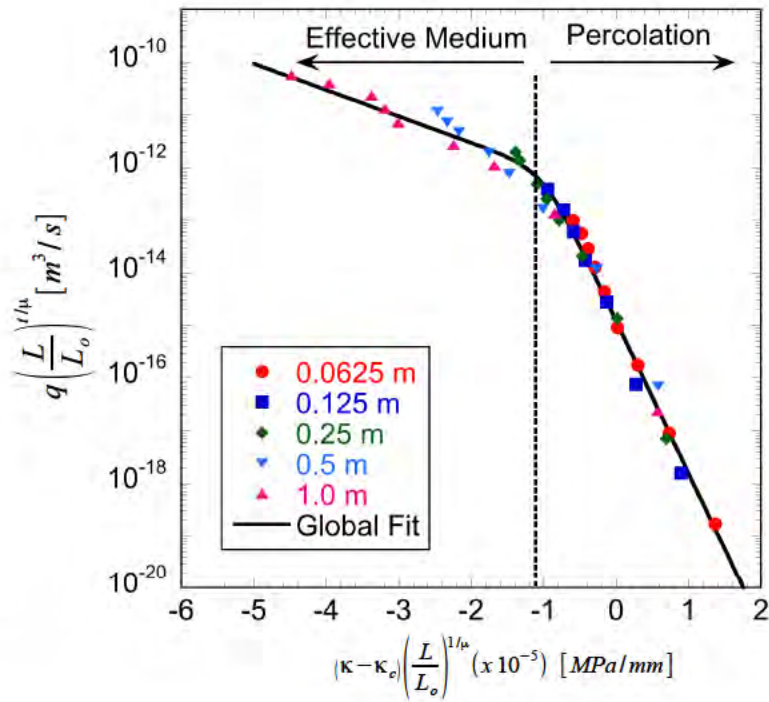


FIG. 3. Universal flow-stiffness function showing a full data collapse. The solid line is provided to guide the eye. The break in slope divides the effective medium regime from the percolation regime

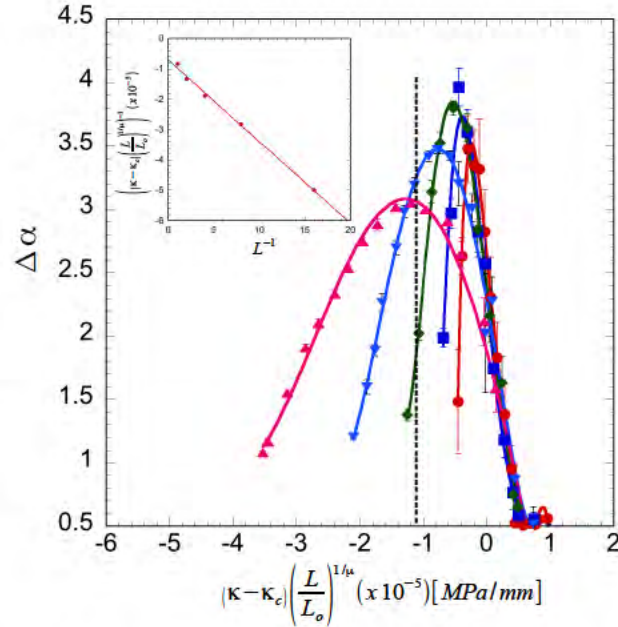


FIG. 4. Width of the multifractal spectrum plotted against the scaled fracture stiffness. Lines are provided to guide the eye. The inset is the extrapolation to infinite scale of the peak in  $\Delta\alpha$ . The symbols and line colors are the same as Figure 3. The dotted line shows the transition between the Effective Medium and Percolation regimes.

2.1. There is a clear break in slope near the abscissa value of -1, with each region above and below this value displaying an exponential dependence. The curve has a slope of -2 for greater values of the abscissa and a slope of -0.5 for lesser values.

We performed a multifractal analysis (see [3] for an overview) of the fluid velocity fields to determine the key geometric feature responsible for the break in slope in the universal function. At low stresses the width,  $\Delta\alpha$ , of the fractal spectrum is small, and the geometry of the fluid speeds exhibits mono-fractal behavior because their statistical moments are distributed nearly homogeneously across the fracture plane. As normal stress increases, the width of the spectrum increases as the moments become inhomogeneous up to stresses associated with the break in scaling at  $(\kappa - \kappa_c)(L/L_0)^{1/\mu} = 10^{-5}$ . At stresses above the break, the multifractal spectrum decreases because the fractures enter the critical regime and the fluid speed is dominated by the “critical necks.” The break in slope of the universal function occurs when the width of the multifractal spectrum is at a maximum (Figure 4). The subplot of Figure 4 extrapolates the inverse of the scaled stiffness at the spectrum peak to the infinite size limit. The peak extrapolates to -1.42 at the infinite limit, which matches the observed break in the universal scaling function.

**4. Discussion.** The data scaling on the universal function displayed in Figure 3 is an important result that connects the hydraulic properties of a weakly correlated fracture (correlation length  $\approx 2\text{mm}$ ) to the fracture specific stiffness; a property that can be probed using remote seismic techniques. The local geometric properties of the system, i.e. “critical necks,” were captured by a universal function that depends on the global transport critical exponent,  $t$ , and the critical stiffness which allowed the system to be written in a scale invariant form. Furthermore, percolation theory was used to derive the geometric scaling exponents from the static cluster statistics of generated fractures. The normal load becomes a key control variable in this study. When the load changes, contact areas are created that alter the cluster statistics of the fracture under load. Rather than the geometry of a fracture completely determining hydraulic properties, the deformation under load must be considered. Thus, fracture specific stiffness can stand in for the void/contact areas because

the stiffness reflects the current state of the topology under the given load conditions.

The system under consideration contains both hydraulic and mechanical properties, and therefore possibly two non-trivial scaling properties. It is well known that the flow rate enters a critical scaling regime near the percolation transition [12]. In addition, the criticality of the mechanical properties were studied and found to have simple scaling with void area fraction. Because of this, a global mechanical scaling exponent is not required to complete the full data collapse, leaving the entire system dependent on the transport exponent,  $t$ . This also means that the fracture specific stiffness can replace the void area fraction as a surrogate, making a strong connection to seismic monitoring techniques.

The two exponential regions in the universal scaling function was an important result from this study. At low stresses, the flow field across the fracture plane is homogeneous. For example, by slicing the field in Figure 1b into smaller regions, the fluid velocity profiles of each subsection will be similar. This implies that the flow covers most of the void spaces of the fracture and is more *sheet-like*. As stress increases, flow paths begin to close, leaving only the main backbone of the original paths. At high stresses, many regions of the void space are without flow leaving only narrow channels that contain flow. If the fracture is sliced as before, there are many regions that have no fluid flow giving the impression of a *string-like* topology. This qualitative description is what the multifractal analysis provides, quantitatively. In this light, the change in slope can be understood as a transition from *sheet-like* to *string-like* topology.

**5. Conclusion.** From this analysis, we conclude that the geometry of a fracture provides all the necessary information to define a scaling relationship between the fracture specific stiffness and the flow rate for weakly correlated fracture aperture geometries. Most fractures are uncorrelated above 5 mm [1]. By conducting a finite-size scaling analysis, we were able to describe the localized fracture properties with a global flow scaling exponent,  $t$ . Incorporating the fracture specific stiffness as a surrogate for void area fraction within the framework of standard percolation theory enabled us to describe the flow-stiffness relationship of fractures with a single universal scaling function. We have demonstrated that the change in slope in the universal function is related to the multifractal spectrum width of the flow speed distribution. However, the values for the slopes of the effective medium and critical regimes remain to be explained. Nonetheless, this universal scaling function provides a stepping-stone to a non-intrusive method to probe the hydraulic properties of single rock fractures in the subsurface. This could provide new methods to determine the future success of subsurface projects. Extending the results here and understanding how stronger correlations affect the scaling is of utmost important because correlated void geometries are often found in nature. This is a subject of continuing research.

**Acknowledgements.** This work is supported by the Geosciences Research Program, Office of Basic Energy Sciences US Department of Energy (DEFG02-97ER14785 08, DE-FG02-09ER16022), by the Geo-mathematical Imaging Group at Purdue University, the Purdue Research Foundation, and from the Computer Research Institute At Purdue University

#### REFERENCES

- [1] S.R. BROWN, R.L. KRANZ, AND B.P. BONNER, *Correlation between the surfaces of natural rock joints*, Geophysical Research Letters, 13 (1986), pp. 1430–1433.
- [2] J.T. CHENG, J.P. MORRIS, J. TRAN, A. LUMSBAINÉ, N.J. GIORDANO, D.D. NOLTE, AND L.J. PYRAK-NOLTE, *Single-phase flow in a rock fracture: micro-model experiments and network flow simulation*, International Journal of Rock Mechanics and Mining Sciences, 41 (2004), pp. 687–693.
- [3] J. FEDER, *Fractals*, Plenum Press, New York, 1988.
- [4] HOPKINS, *The Effect of Surface Roughness on Joint Stiffness, Aperture, and Acoustic Wave Propagation*, PhD thesis, 1990.
- [5] J.C. JAEGER, N.G.W. COOK, AND R.W. ZIMMERMAN, *Fundamentals of Rock Mechanics*, Blackwell Publishing, 4th ed., 2007.
- [6] C.G. LAMBERT, *Multipole-Based Algorithms for Efficient Calculation of Forces and Potentials in Macroscopic Periodic Assemblies of Particles*, PhD thesis, 1994.